Short Papers

A Semidistributed HEMT Model for Accurate Fitting and Extrapolation of S-Parameters and Noise Parameters

M. T. Hickson, P. Gardner, and D. K. Paul

Abstract—**A model is described for a low noise mm-wave HEMT device. It takes account of the distributed nature of the gate and drain electrodes by dividing the active region of the device into a number of slices. Each slice is modelled as an intrinsic HEMT with thermal noise sources and the slices are connected together through lossy reactances. The parameters of the first slice are made different from those of the remaining slices, in order to account for the inevitable differences in the field distribution in the gate feed region. The model parameters have been optimized numerically to fit the manufacturer's measured S-parameters and all four noise parameters, for a commercially available HEMT chip. A good fit has been achieved simultaneously to all of these parameters, and the model therefore provides a reasonable basis for extrapolation to higher frequencies. The significance of the distributed gate effect and the unequal slice effect are assessed by comparing the best fit achievable when these effects are not included.**

Introduction

Accurate design of low noise GaAs FET or HEMT amplifier circuits demands an accurate knowledge of the scattering parameters and all four noise parameters, as functions of frequency, for the chosen active device, over the frequency range of interest. Values for all the required parameters can be determined by measurement, but this is very difficult to do accurately, especially in the case of noise parameters in the millimeter wave region. A device model with a realistic physical basis is therefore of value as a tool for extrapolating from lower frequency measured results.

Many authors have reported work on GaAs FET and HEMT device signal and noise models. The approaches may be divided broadly into those based on fundamental physical properties of the device [1]–[4], and those which add appropriate noise sources to an equivalent circuit model to fit the measured noise parameters [5]–[8]. The paper by Pospieszalski [9] essentially falls into the second category, although the method used may also serve to provide some insight into the physical origin of the noise sources. Pospieszalski demonstrated that his model could be used to give an accurate prediction of the noise parameters of a particular HEMT from 4 GHz to 20 GHz, on the basis of two frequency independent equivalent temperatures, extracted from measurements at a single frequency, 8.5 GHz.

To model the signal and noise properties at higher frequencies, several authors have included the effects of the distributed nature of the gate and drain electrodes, with or without mutual coupling, in their models [10]–[12]. A recent paper by Escotte and Mollier [11] describes a sliced model, in which the distributed effects are accounted for by dividing the active region of a GaAs FET along its width into a number of equal slices, each of which is modelled as an intrinsic FET. The slices were connected together through reactive elements with parasitic resistances, to give a discretized approximation of the distributed electrode effect, ignoring mutual coupling.

Using this model they predicted the minimum noise figure of a GaAs FET up to 40 GHz and showed that a significant departure from the Fukui formula [6] could be expected for that particular device above 36 GHz. They also state that the other three noise parameters can be determined from the model, although they do not give actual values.

In this paper we report a signal and noise model which adopts the intrinsic device model of Pospieszalski [9], within a sliced FET structure similar to that used by Escotte and Mollier [11]. A new feature introduced in our model is that the parameters of the first slice are allowed to differ from those of the remaining slices, in order to account for possible differences in the field structure in the gate feed region. We have found that this model allows significant improvements in the simultaneous fitting of the S-parameters and all four noise parameters for a commercially available HEMT device.

Details of the Modified Sliced Model

The overall structure of the model is shown in Fig. 1. Any number of slices can be used. The number should be chosen such that the physical length of each slice is short compared to the guided wavelength on the gate and drain electrode transmission lines, at the maximum frequency for which the model is to be used. In the example considered here, five slices were used. In the optimization process, slices two to five inclusive were constrained to be identical, whilst slice one was allowed to differ in order to account for differences in the field structure in the gate feed region. To make the notional width of all five slices identical, however, they were all constrained to have the same value of transconductance, g_m.

The detailed structure of an individual slice is shown in Fig. 2. This model is similar to that used by Pospieszalski [9], with the addition of a small resistance in series with the gate to drain feedback capacitance, to account for ohmic losses associated with this feedback path. The individual temperatures of the resistances in the model were allowed to vary in the optimization.

Optimization and Results

The model was optimized to fit the manufacturer's measured S-parameters from 2 to 40 GHz, and the noise parameters from 14 to 26 GHz, for the TOSHIBA HEMT chip, type JS8900-AS. The optimization was carried out using the linear analysis functions of the CAD package LIBRA [13]. The optimization process was configured to minimize the error function, E, given by

$$E = \sum_{f=2}^{40} \sum_{i=1}^{2} \sum_{j=1}^{2} |S_{ij}^{M}(f) - S_{ij}(f)|^2 + \sum_{\substack{f=14,18,\\22,24,\\26}} [(F_{\min}^{M}(f) - F_{\min}(f))^2 + |\Gamma_{\mathrm{OPT}}^{M}(f) - \Gamma_{\mathrm{OPT}}(f)|^2 + (r_n^{M}(f) - r_n(f))^2]$$

Manuscript received September 18, 1991; revised January 7, 1992.

The authors are with the Department of Electrical Engineering & Electronics, The University of Manchester Institute of Science & Technology, P.O. Box 88, Manchester, M60 1QD, United Kingdom.

IEEE Log Number 9200859.

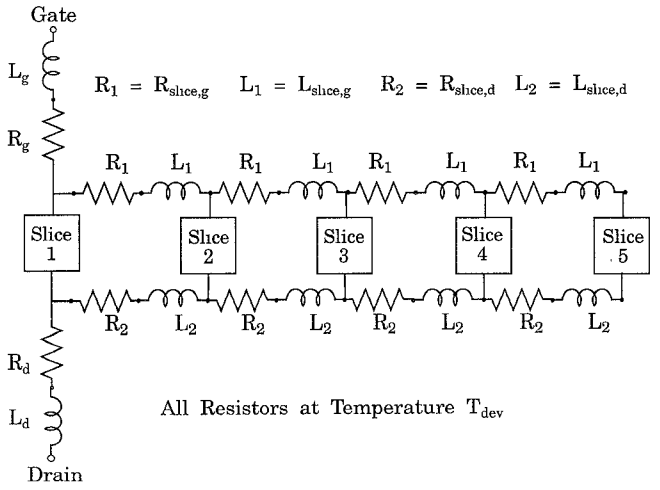

Fig. 1. Overall structure of sliced model.

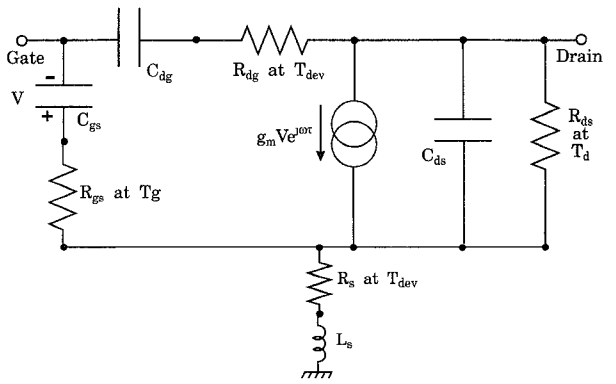

Fig. 2. Individual slice structure of sliced model.

where

$S_{ij}(f)$ are the elements of the common source scattering parameter matrix at frequency f GHz,
$F_{min}(f)$ is the minimum noise figure,
$\Gamma_{OPT}(f)$ is the source reflection coefficient for optimum noise figure,
$r_n(f)$ is the equivalent noise resistance.

The superscript M denotes predictions of the model whilst the parameters shown without superscripts are the measured results for the device.

The circuit element values and temperatures resulting from the optimization are shown in Tables I and II. The signal and noise parameters of the model are shown in Figs. 3 to 7, along with the manufacturer's measured results. The legends for Figs. 3 to Fig. 7 are given in Table III.

The S-parameters (Figs. 3 and 4) show good agreement over the full 2 to 40 GHz range, and the noise parameters (Figs. 5 to 7) show good agreement up to 26 GHz, the highest frequency for which the manufacturer provides full data. The model thus serves as a reasonable basis for extrapolation of noise parameters beyond 26 GHz and of S-parameters beyond 40 GHz.

Discussion

The significance of the distributed and unequal slice effects can be assessed by comparison with the best fit achieved using a similar model with only a single slice and the same optimization procedure. The optimization results for such a non-distributed model are also shown in Figs. 3 to 7. As a measure of the difference, the minimum error function terms achieved with both models are plotted against frequency in Fig. 8, showing that the non-distributed model has a larger error over the whole frequency range, with particularly marked differences at lower frequency. It can be seen from Fig. 7 that a large contribution to this difference is brought about by the poor modelling of r_n by the non-distributed model below 14 GHz. Noise parameters below 14 GHz were not included in the error function for the optimization. This suggests that in the non-distributed model the circuit parameter values were adjusted un-

TABLE I
Parameters of FET Slices

Parameter	First Slice	Slices 2 to 5
T_g	1.0°C	69.1°C
T_d	188.3°C	1589.1°C
C_{gs}	0.0313 pF	0.0223 pF
R_{gs}	5.65 Ω	42.0 Ω
L_s	0.153 nH	0.035 nH
R_s	32.1 Ω	2×10^{-6} Ω
C_{ds}	0.0614 pF	0.03 fF
R_{ds}	3160.9 Ω	809.8 Ω
R_{dg}	0.0570 Ω	0.0130 Ω
C_{dg}	0.0051 pF	0.0071 pF

TABLE II
Common Parameters

Parameter	Value
T_{dev}	25.5°C
$R_{slice,g}$	0.0114 Ω
$L_{slice,g}$	0.0127 nH
$R_{slice,d}$	0.0320 Ω
$L_{slice,d}$	0.0184 nH
R_g	0.0936 Ω
L_g	0.128 nH
R_d	1.664 Ω
L_d	0.0371 nH
g_m	0.0102 Ω^{-1}
τ	4.126 ps

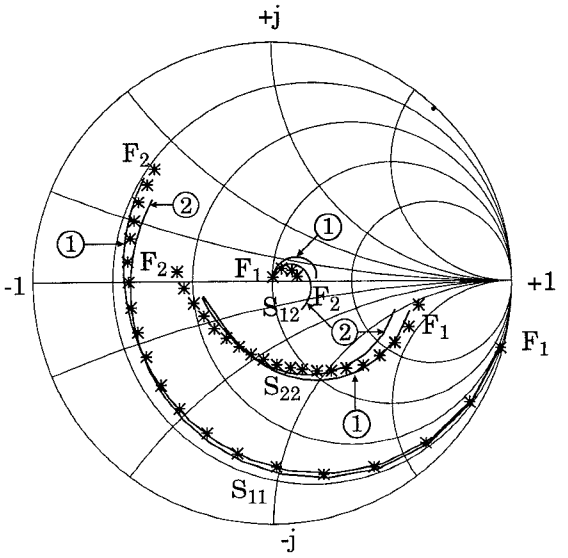

Fig. 3. Measured and modelled S-parameters, S_{11}, S_{12}, S_{22}.

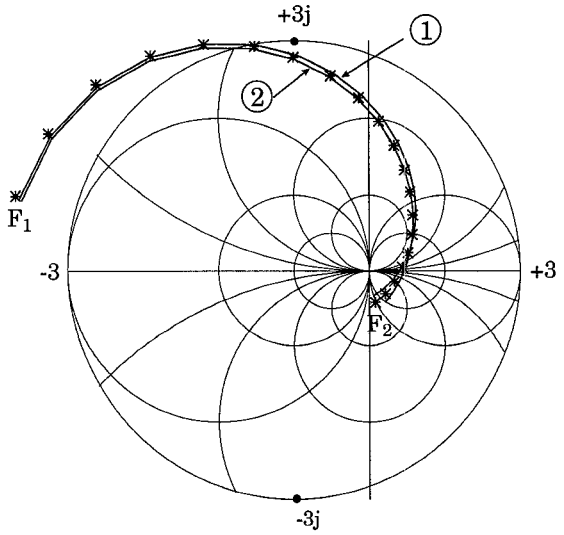

Fig. 4. Measured and modelled S-parameter, S_{21}.

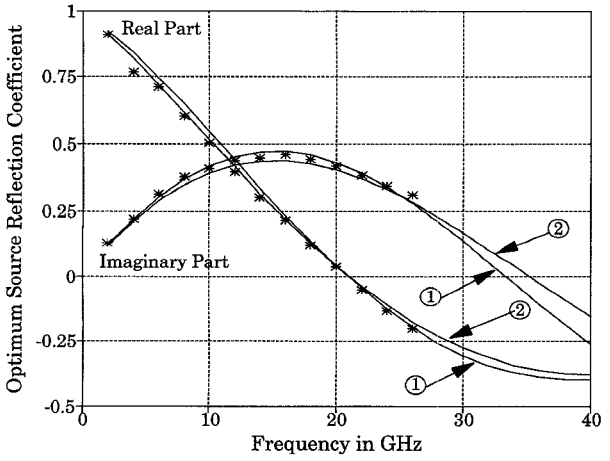

Fig. 5. Measured and modelled optimum noise match.

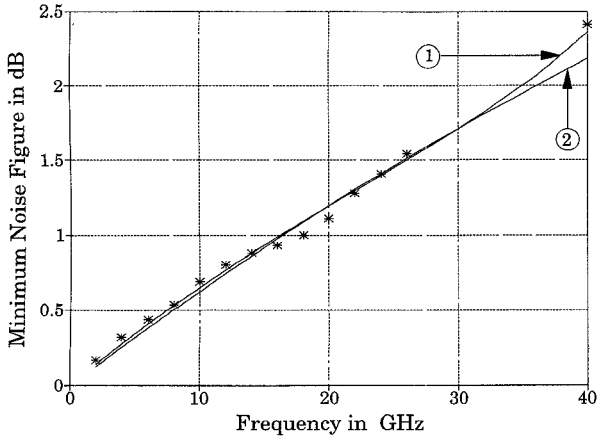

Fig. 6. Measured and modelled minimum noise figure.

realistically in order to fit high frequency effects, whereas in the sliced model these effects are accounted for in the structure of the model, and a good fit to lower frequency measurements arises naturally.

It can be seen from Fig. 6 that the predicted optimum noise figure at higher frequencies is higher when the distributed effect is

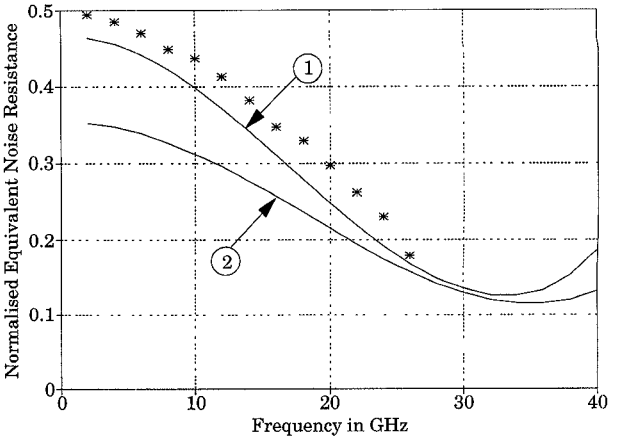

Fig. 7. Measured and modelled normalized equivalent noise resistance.

TABLE III
LEGENDS FOR FIGS. 3–7

F_1 = 2 GHz : F_2 = 40 GHz
① = sliced model data
② = unsliced model data
* = measured data

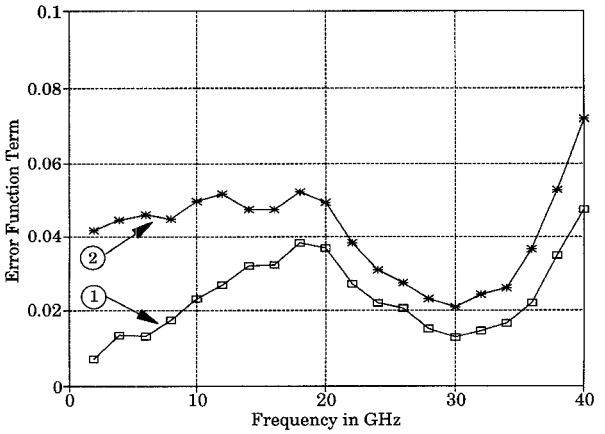

Fig. 8. Frequency dependence of error function term.

included. This agrees with the results in [11] and [12], and also with the manufacturer's measurement of F_{min} at 40 GHz. The non-distributed model shows a tendency for the gradient of F_{min} with frequency to reduce at higher frequencies, which is clearly contrary to measured results. A striking feature of Fig. 7 is the greatly improved fitting of the equivalent noise resistance in the new model. As noted by Fukui [7], this is a parameter of great importance in broadband low noise amplifier design.

The temperature parameters arising from the optimization are similar to those reported by Pospieszalski [9] in that the gate temperatures are close to ambient temperature, whilst the drain temperatures are significantly higher. The effective temperatures of the parasitic resistances are also close to ambient, which is reasonable since only ambient thermal noise arises in these elements.

The significance of the unequal slice effect alone can be judged by studying the difference made by the optimizer to the parameters of the first slice. The optimization method described is probably insufficiently powerful to determine so many parameters accurately and uniquely in an ill-conditioned model of this type [14]. For example, Pospieszalski [9] showed that even for a non-distributed

model, it is possible to change one element (R_{gs}) and then to compensate others to reestablish a good fit. However, the fact that an improved fit is achieved when the first slice is allowed to differ suggests that there are significant differences in the field structure in the gate feed region. In particular, the source resistance is large in the first slice and negligible in the remainder. This could be associated with the perturbation of the channel near the source by the gate feed. A model based more directly on the underlying physics of the device would be necessary in order to quantify these differences accurately.

Conclusion

It has been shown that an improvement in fitting of a HEMT device model to measured signal and noise parameters can be brought about by using a sliced model to account for the effects of the distributed nature of the gate and drain electrodes, and by allowing the first slice to differ from the others in order to account for the difference in field structure in the gate feed region.

Acknowledgment

We wish to thank the UK Science and Engineering Research Council for a research studentship for M. T. Hickson.

References

[1] R. A. Pucel, H. A. Haus, and H. Statz, "Signal and noise properties of GaAs microwave FET," in *Advances in Electronics and Electron Physics*, vol. 38, L. Morton, Ed. New York: Academic Press, 1975.
[2] T. M. Brookes, "The noise properties of high electron mobility transistors," *IEEE Trans. Electron Devices*, vol. ED-33, pp. 52–57, Jan. 1986.
[3] A. Cappy, A. Vanoverschelde, M. Schortgen, C. Versnaeyen, and G. Salmer, "Noise modelling in submicrometer-gate two-dimensional electron gas field effect transistors," *IEEE Trans. Electron Devices*, vol. ED-32, pp. 2787–2795, Dec. 1985.
[4] C. Moglestue, "A Monte Carlo particle study of the intrinsic noise figure in GaAs MESFET," *IEEE Trans. Electron Devices*, vol. ED-32, pp. 2092–2096, Oct. 1985.
[5] H. Fukui, "Design of Microwave GaAs MESFETs for broadband, low-noise amplifiers," *IEEE Trans. Microwave Theory Tech.*, vol. MTT-27, pp. 643–650, July 1979.
[6] H. Fukui, "Optimal noise figure of microwave GaAs MESFETs," *IEEE Trans. Electron Devices*, vol. ED-26, pp. 1032–1037, July 1979.
[7] A. F. Podell, "A functional GaAs FET noise model," *IEEE Trans. Electron Devices*, vol. ED-28, pp. 511–517, May 1981.
[8] M. S. Gupta and P. T. Greiling, "Microwave noise characterization of GaAs MESFETs: Determination of extrinsic noise parameters," *IEEE Trans. Microwave Theory Tech.*, vol. 36, pp. 745–751, Apr. 1988.
[9] M. W. Pospieszalski, "Modeling of noise parameters of MESFETs and MODFETs and their frequency and temperature dependence," *IEEE Trans. Microwave Theory Tech.*, vol. 37, pp. 1340–1350, Sept. 1989.
[10] W. Heinrich, "Limits of FET modelling by lumped elements," *Electron. Lett.*, vol. 22, pp. 630–632, June 1986.
[11] L. Escotte and J. Mollier, "Semidistributed model of millimeter-wave FET for *S*-parameter and noise figure predictions," *IEEE Trans. Microwave Theory Tech.*, vol. 38, pp. 748–753, June 1990.
[12] C. H. Oxley and A. J. Holden, "Simple models for high-frequency MESFETs and comparison with experimental results," *Proc. Inst. Elec. Eng.*, vol. 133, pt. H, pp. 335–340, Oct. 1986.
[13] *Touchstone and Libra User's Guide*, EEsof Inc., USA, July 1989.
[14] A. D. Patterson, V. F. Fusco, J. J. McKeown, and J. A. C. Stewart, "Problems associated with small signal MESFET equivalent circuit model parameter extraction," in *Dig. 14th ARMMS Conf.*, Queens University, Belfast, Mar. 1991.

Accurate Modeling of Axisymmetric Two-Port Junctions in Coaxial Lines Using the Finite Element Method

Waymond R. Scott, Jr.

***Abstract*—A technique is developed for analyzing axisymmetric two-port junctions (axisymmetric discontinuities) in coaxial lines using the finite element method. Boundary conditions are developed for the input and output ports that absorb the reflected and transmitted waves while injecting the incident wave. The use of higher order elements is shown to greatly improve the accuracy, i.e., the accuracy increases rapidly with the order of the elements even when the number of nodes is kept roughly constant. The accuracy of the technique is verified by comparison with the theoretical and experimental results of other investigators for three discontinuities, and the agreement is shown to be excellent.**

Introduction

Discontinuities in coaxial lines are part of many microwave devices. Accurate models of these discontinuities are needed in the design of the devices. Traditionally the discontinuities have been modeled using mode matching and variational techniques; however, these techniques require a significant amount of analytical analysis for each geometry and become very complex for all but relatively simple geometries.

In this work, the finite element method (FEM) will be used to accurately model axisymmetric two-port junctions (axisymmetric discontinuities) in coaxial lines. The flexibility of the FEM allows more complicated geometries to be modeled. The addition of materials into the junction and complex geometrical shapes do not add any complications to the analysis. Furthermore, very accurate results are obtainable with the FEM with reasonable computational efficiency when higher order elements are used. To demonstrate the flexibility and the accuracy obtainable with the FEM, three discontinuities are analyzed, and the results are compared to theoretical and experimental results of other investigators. The agreement is shown to be excellent; even though in each of these discontinuities, the fields are singular at a corner on the center conductor and no special analysis is performed in this work to take the singularities into account. For one of the cases, the accuracy versus the order of the elements from first to fourth order is investigated.

This work compliments the work of other investigators who have used the FEM to investigate axisymmetric problems: Marouby *et al.* [1] and Wilkins *et al.* [2] have investigated transitions between coaxial lines; and Silvester and Konrad [3], [4] and Daly [5] have investigated the modes in axisymmetric resonators.

Formulation

Fig. 1 is a schematic diagram of a general coaxial discontinuity in which the region to be modeled with the FEM is indicated. For this analysis, the incident wave is assumed to be a TEM mode. The

Manuscript received September 10, 1991; revised January 14, 1992. This work was supported in part by the Georgia Tech Material Metrology Consortium, the Georgia Tech Manufacturing Research Center, and the Joint Services Electronics Program under Contracts DAAL 03-87-K-0059 and DAAL-03-90-C-0004.

The author is with the Georgia Institute of Technology, School of Electrical Engineering, Atlanta, GA 30332.

IEEE Log Number 9200860.